



Cite this: DOI: 10.1039/d5cc02611c

Received 8th May 2025,
Accepted 23rd June 2025

DOI: 10.1039/d5cc02611c

rsc.li/chemcomm

In situ oxidizable directing group-enabled enantioselective synthesis of chiral platform ferrocene formaldehydes†

Devendra Parganiha,¹ Ashwini Dilip Dhumale,¹ Yagya Dutt Upadhyay,¹
Vishal Choudhary,¹ Svastik Jaiswal,¹ Raushan Kumar Jha¹ and Sangit Kumar^{1*}

Herein, we have developed an efficient oxidatively removable directing group approach, enabling highly enantioselective Pd^{II}-catalyzed C–H activation. Successful rationalization of difficult C–H activation over the labile β–H oxidation step led to the direct synthesis of chiral 2-alkenylated ferrocene formaldehydes with up to 71% yields and 98 : 2 er.

The integration of directing groups (DGs) into transition metal-catalysed C–H activation has revolutionized organic synthesis, as these directing groups not only lead to a new array of molecules but also stabilize the inherently unstable species.¹ However, *in situ* transformation of the directing group into desired functionalities is always challenging and has not been fully addressed yet.¹

Planar chiral ferrocenes,² particularly ferrocene formaldehydes, serve as important platform building blocks for synthesizing various planar chiral catalysts and ligands, including industrially used Josiphos, Ugi's amines, PPFA, and PHOX-type ligands (Scheme 1).³ Synthesis of planar chiral ferrocene formaldehyde derivatives has always been challenging yet remains essential.⁴ The major limitations are the multistep conventional routes or expensive reagents for the very high enantioselective synthesis of platform ferrocene formaldehydes.⁴ Moreover, a Pd^{II}-enabled transient directing group approach⁵ for highly enantioselective C–H activation was unsuccessful for metallocenes as it led to C–H activation on the lower cp-ring.⁵

Our group is continuously working on TM-catalyzed directing group methodologies for diverse selective C–H activation in ferrocenes.⁶ Furthermore, we aim to develop a highly enantioselective and efficient methodology to construct important chiral platform ferrocene formaldehydes with high enantioselectivity. Consequently, a removable directing group strategy was envisioned, leading to enantioselective C–H activation and,

subsequently, *in situ* transformation of the directing group into important platform chiral formaldehyde functionalities (Scheme 1). Herein, we have successfully developed an *in situ* oxidizable directing group methodology through a sequential rationalization of unreactive enantiotopic C–H bond activation over facile β–H oxidation of protic amines. The developed *in situ* oxidizable directing group methodology led to the efficient synthesis of diverse new alkenylated platform chiral ferrocene formaldehydes with up to 71% yield and 98 : 2 er in a step-economical manner (Scheme 1).

We commenced our investigation of ferrocenyl-methylamine **1a** with a combination of Pd(OAc)₂ as a catalyst and a recently reported chiral NOBINAc ligand^{6c} with acrylate **2a** (Table 1). In addition, an oxidant, Cu(OAc)₂, with the base Cs₂CO₃, was added to facilitate the subsequent oxidation of the catalyst as well as the directing group. Ferrocenylamine **1a** produced the desired oxidized amine product – chiral 1,2-alkenylated ferrocene formaldehyde **3a** – in a poor yield of 20% with a moderate enantioselectivity of 90 : 10 er (Table 1, entry 1). Furthermore, various solvents were screened to control the excessive oxidation of amine **1a** (Table 1, entries 2–4). Among the solvents screened, *tert*-amyl alcohol increased the yield of **3a** to 32%, and undesirably the enantioselectivity of **3a** was reduced to 70 : 30 er (Table 1, entry 4), which may be due to the incompatibility of the NOBINAc ligand with the polar protic *tert*-amyl alcohol.⁷ To circumvent the undesired oxidation of **3a** to FcCHO and to further enhance the er, we screened a series of chiral mono-protected amino acid ligands (**L2–L9**; see Fig. S3 and Table S2, ESI†). To our delight, the screened MPAA ligands **L2–L9** demonstrated notable efficacy, delivering yields ranging from 32% to 75% and er values from 87 : 13 to 98 : 2. Among all the ligands screened, Boc-*L*-*tert*-Leucine **L2** provided the best results with amine **1a**, achieving a 75% yield and 98 : 2 er of **3a** (for details see Tables S1–S4, ESI†).

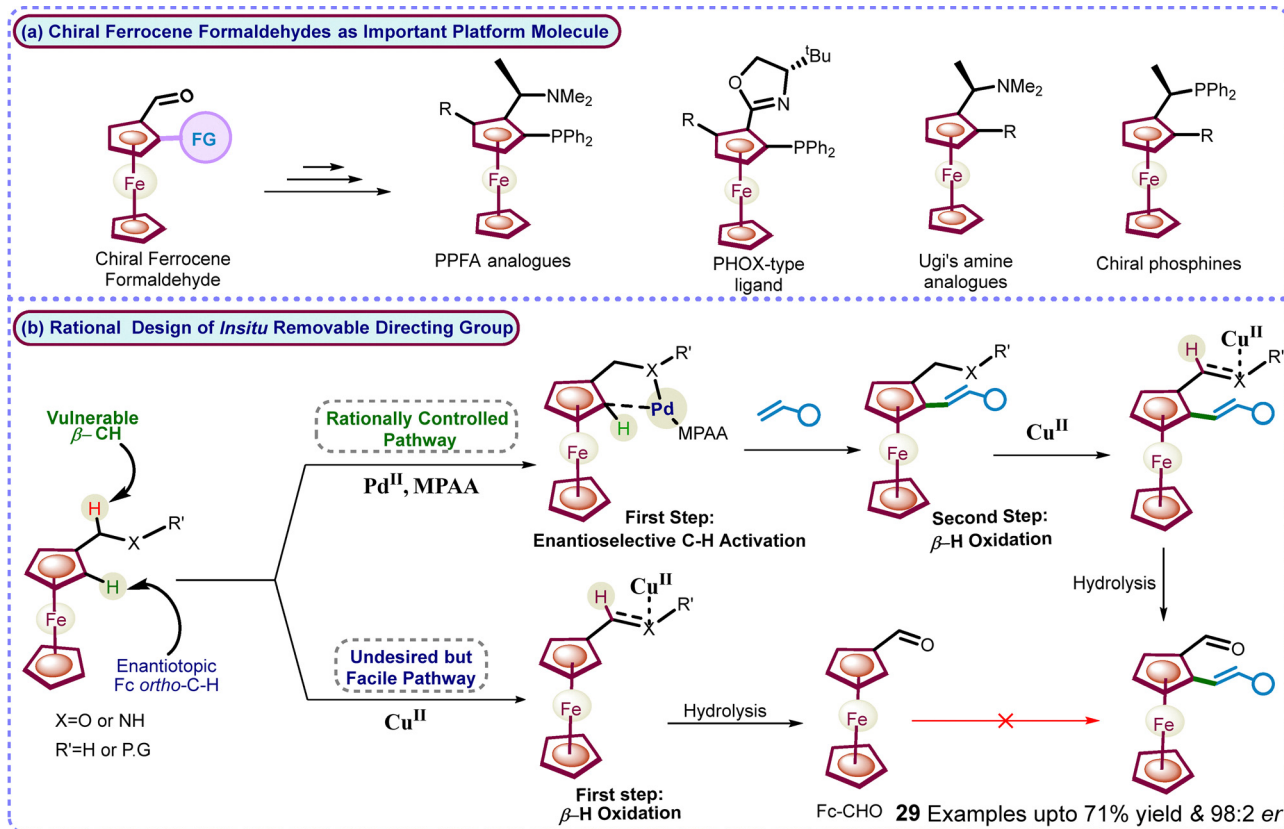
Next, a variety of ferrocenylamines **1b–1h** were tested under enantioselective C–H activation followed by oxidative deamination conditions (Fig. 1). Other sulfonyl (SO₂R)-protected

Department of Chemistry, Indian Institute of Science Education and Research
Bhopal, Bhopal By-Pass Road, Bhopal, Madhya Pradesh 462066, India.

E-mail: sangitkumar@iiserb.ac.in

† Electronic supplementary information (ESI) available. See DOI: <https://doi.org/10.1039/d5cc02611c>





Scheme 1 (a) Ferrocene formaldehyde as a valuable platform molecule and (b) rational design of the step-economical oxidizable directing group strategy and our work.

Table 1 Optimization of reaction conditions for the enantioselective *in situ* oxidizable directing group strategy

Entry ^a	Solvent	Ln	FcCHO (%)	3a ^b (%)	er ^c (%)
1	THF	L1	80	20	90:10
2	Toluene	L1	75	25	87:13
3	DMF	L1	88	12	76:24
4	^t Amyl alcohol	L1	68	32	70:30
5	^t Amyl alcohol	L2	35	65	96:4
6 ^d	^t Amyl alcohol	L2	25	75	98:2

^a Reaction conditions: **1a** (0.1 mmol), **2a** (0.2 mmol), Pd(OAc)₂ (0.01 mmol), ligand (0.04 mmol), Cs₂CO₃ (0.2 mmol), Cu(OAc)₂ (0.15 mmol), DMSO (0.5 mmol), dry solvent (1 mL), air, 60 °C, 24 h. ^b The crude yield of **3a** was determined by ¹H NMR with CH₂Br₂ as an internal standard. ^c The enantiomeric ratio (*er*) of **3a** was determined by HPLC analysis. ^d The reaction was stirred for 30 h at 55 °C. Ligand **L1** = NOBINAc and **L2** = Boc-L-tert-leucine.

ferrocenylamines **1b–1e** also provided the chiral product **3a** in 5–55% yields, with 88:12 to 98:2 *er*, whereas amines **1f–1h**, lacking a coordinating SO₂R group, did not yield the desired

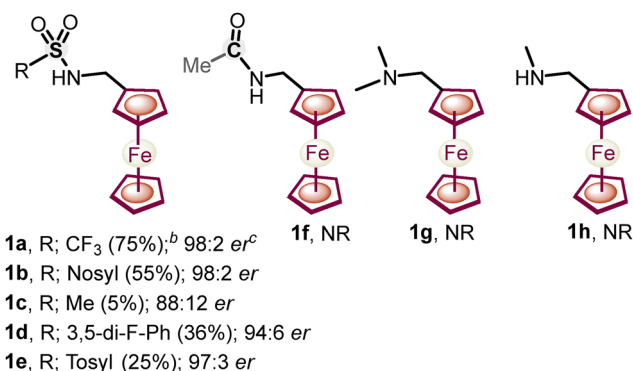
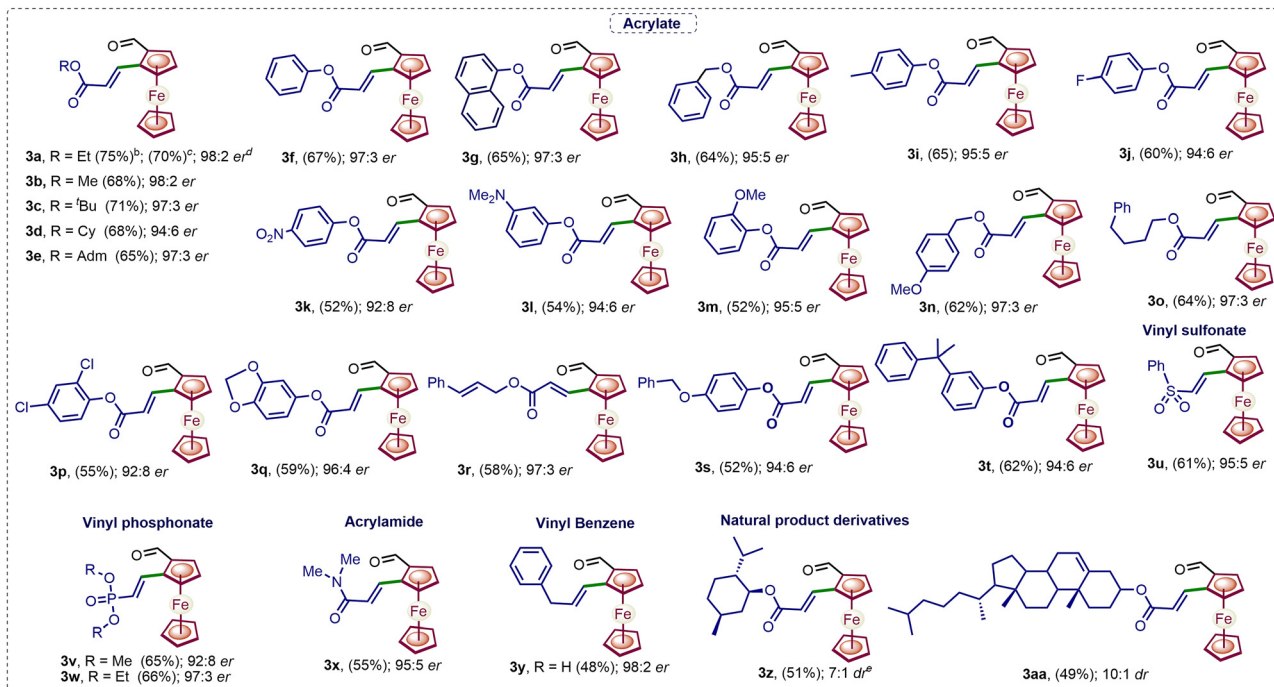


Fig. 1 Screening of amines for enantioselective C–H activation and subsequent oxidative deamination. Reaction conditions: the same as those mentioned in Table 1, entry 6.

alkenylated formaldehyde **3a**. The screening of the various amines suggests that the low p*K*_a of the methylene C–H bond, the coordinating ability of amine DGs, and the better leaving group ability of the –S(O)₂R substituent are needed for effective enantioselective C–H activation and *in situ* directing group removal.⁸ Furthermore, the substrate scope with regard to various olefins (**2a–2aa**) was explored. Acrylates **2a–2t** with alkyl, electron-donating and electron-withdrawing group-substituted aryl, naphthyl, and benzyl substitution yielded an



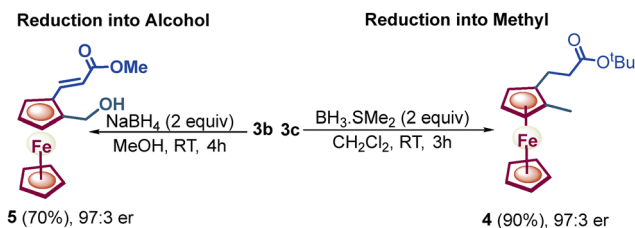


Scheme 2 Substrate scope for enantioselective C–H alkenylation. ^a Reaction conditions are the same as those mentioned in Table 1, entry 6. ^b The crude yield of **3a** was determined by ¹H NMR with CH₂Br₂ as an internal standard. ^c Isolated yields of 1,2-alkenylated ferrocene formaldehydes **3a–3aa**. ^d The *er* of **3a** was determined by HPLC. ^e The *dr* ratio of the isolated product was determined by ¹H NMR.

array of 1,2-alkenylated ferrocene formaldehydes **3a–3t** in 52–71% yields and 92:8–98:2 *er* (Scheme 2). Moreover, other olefins, namely, vinyl sulfonate **2u**, phosphonates **2v** and **2w**, acrylamide **2x**, and vinyl benzene **2y**, also showed the amenability to afford respective chiral 1,2-alkenylated ferrocene formaldehydes **3u–3y** in 48–66% yields and 92:8–97:3 *er* (Scheme 2). Furthermore, olefins derived from natural products *L*-menthol and cholesterol **2z** and **2aa** were also coupled diastereoselectively to afford the respective menthol- and cholesterol-containing chiral ferrocene formaldehydes **3z** and **3aa** in 51% and 49% yields, with 7:1 to 10:1 *dr*, respectively (Scheme 2). Additionally, we performed a gram-scale reaction, achieving up to 50% yield of chiral 1,2-alkenylated ferrocene formaldehyde **3a** with 95:5 *er*. Furthermore, chiral 1,2-alkenylated ferrocene formaldehydes **3c** and **3b** were reduced to their respective methyl and alcohol groups, leading to molecules **4** and **5** without any reduction in enantioselectivity (**3c**, 97:3 *er* *versus* **4**, 97:3 *er*, and **3b**, 97:3 *er* *versus* **5**, 97:3 *er*, Scheme 3).

Furthermore, to gain mechanistic insights into controlled amine oxidation *versus* enantioselective C–H activation pathways, a series of control experiments were performed (Scheme 4).

The failure to obtain product **3a** from ferrocene formaldehyde under optimized conditions (Scheme 4, eqn (1)) rules out imine involvement in the enantioselective C–H activation. Furthermore, we examined the possibility of a radical-driven process where the radical quenchers (TEMPO and BHT) failed to prevent oxidation or to form any adducts as observed by mass spectrometry (Scheme 4, eqn (2)). Next, the role of Pd^{II} and Cu^{II} in the oxidation of amine was studied by selectively

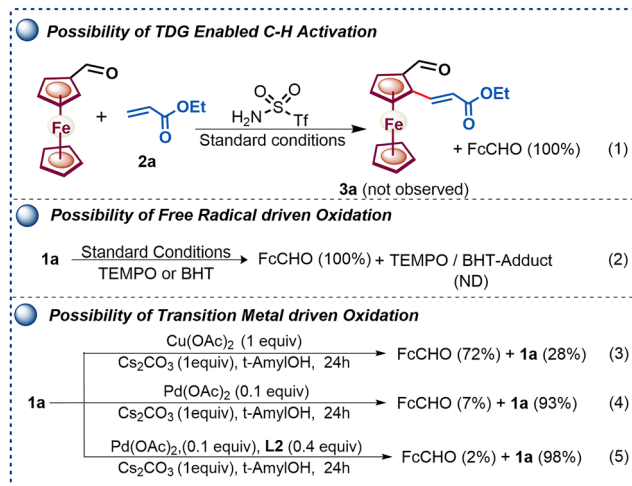


Scheme 3 Post-derivatization of aldehydes into methyl and alcohol functionalities.

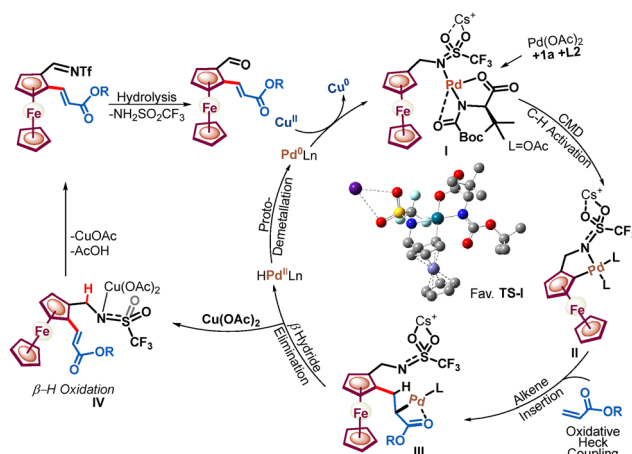
varying the metal salts involved in the reaction (Scheme 4, eqn (3)–(5)). The reaction outcomes indicate that both Cu(OAc)₂ and Pd(OAc)₂ are capable of facilitating the respective β-H oxidation, and the presence of the base Cs₂CO₃ significantly accelerates the oxidation.

Additionally, it was noted that the presence of an MPAA ligand slows the β-H oxidation driven by the Pd(OAc)₂ catalyst (Scheme 4, eqn (5)). Furthermore, the relative rates of C–H activation *versus* amine oxidation were rationalized by ¹H NMR experiments, suggesting that the rate of C–H activation is 1.76 times higher than the rate of amine oxidation (see Fig. S4–S9, ESI†). Further, a ligand acceleration experiment was conducted, which revealed that the presence of ligand **L2** accelerates the reaction by 4.6-fold (see Fig. S8, ESI†). Furthermore, the DFT computational studies were performed to determine the relative enantiotopic C–H energy within CMD, which showed a 2.48 kcal mol^{−1} lower energy for the favorable TS than for the unfavorable TS (see Fig. S10, ESI†). Based on control experiments, we have proposed a plausible catalytic cycle (Scheme 5). Initially, amine





Scheme 4 Mechanistic investigation of C–H activation versus deamination.



Scheme 5 Plausible catalytic cycle. The favourable TS shown was obtained by DFT calculations.

1a, Pd(OAc)_2 , and ligand **L2** with a Cs^+ cation form a Pd-amine, **I**, as suggested by ^{19}F NMR experiments (see Fig. S9, ESI †) and a previous report.¹⁰ Furthermore, the Pd-amine **I** undergoes enantioselective C–H activation to generate a chiral palladacycle, **II**. The chiral palladacycle **II** interacts with the olefin through π -bond interactions, leading to the formation of a Pd-alkyl intermediate, **III**. Consequently, intermediate **III** would undergo β -H elimination to afford chiral 2-alkenylated ferrocenylamine. The 2-alkenylated ferrocenylamine was then oxidized by Cu(OAc)_2 through one-electron oxidation of triflamide to form copper-amidate **IV**, followed by hydrolysis, yielding chiral 2-alkenylated ferrocenyl formaldehydes.⁹

In summary, we have developed a mild *in situ* oxidizable directing group methodology for the highly enantioselective and monoselective synthesis of chiral platform ferrocene formaldehydes. The developed methodology effectively rationalizes the difficult enantioselective C–H activation step first and the facile β -H oxidation step later, which represents an efficient alternative to the transient directed strategy using a dual $\text{Pd}^{\text{II}}/\text{Cu}^{\text{II}}$ cycle in stacked molecules.

SK acknowledges DST-ANRF (CRG/2023/002473), New Delhi, and IISER Bhopal for financial support. DP and SJ acknowledge the UGC,

New Delhi, for fellowships [NTA ref. no. 191620241186] and [NTA ref. no. 201610131472]. AD acknowledges DST INSPIRE (IF210534) for the fellowship.

Conflicts of interest

There are no conflicts to declare.

Data availability

Detailed synthetic procedures, reaction condition optimization, data characterization, controlled experiments, and geometries and energies of theoretically investigated structures are provided in the ESI. †

Notes and references

- (a) S. Murai, F. Kakiuchi, S. Sekine, Y. Tanaka, A. Kamatani, M. Sonoda and N. Chatani, *Nature*, 1993, **366**, 529–531; (b) C. Sambigao, D. Schonbauer, R. Blicke, T.-D. Huy, G. Pototschnig, P. Schaaf, T. Wiesinger, M. F. Zia, J.-W. Delord, T. Besset, B. U. W. Maes and A. Schnurch, *Chem. Soc. Rev.*, 2018, **47**, 6603–6743; (c) G. Liao, T. Zhang, Z.-K. Lin and B.-F. Shi, *Angew. Chem., Int. Ed.*, 2020, **59**, 19773–19786; (d) R. L. Carvalho, R. G. Almeida, K. Murali, L. A. Machado, L. F. Pedrosa, P. Dolui, D. Maiti and E. N. D. S. Júnior, *Org. Biomol. Chem.*, 2021, **19**, 525–547; (e) L. Guillemard, N. Kaplaneris, L. Ackermann and M. J. Johansson, *Nat. Rev. Chem.*, 2021, **5**, 522–545; (f) R. S. Thombal, P. Yuosef, M. Rubio, D. Lee, D. Maiti and Y. R. Lee, *ACS Catal.*, 2022, **12**, 5217–5230; (g) B. B. Zhan, L. Jin and B.-F. Shi, *Trends Chem.*, 2022, **4**, 220–235; (h) Q. Zhang, L.-S. Wu and B.-F. Shi, *Chem*, 2022, **8**, 384–413; (i) K. Wu, N. Lam, D. A. Strassfeld, Z. Fan, J. X. Qiao, T. Liu, D. Stamos and J.-Q. Yu, *Angew. Chem., Int. Ed.*, 2024, **63**, e202400509.
- (a) D.-W. Gao, Q. Gu, C. Zheng and S.-L. You, *Acc. Chem. Res.*, 2017, **50**, 351–365; (b) Z.-J. Cai, C.-X. Liu, Q. Wang and S.-L. You, *Nat. Commun.*, 2019, **10**, 4168; (c) C.-X. Liu, Q. Gu and S.-L. You, *Trends Chem.*, 2020, **2**, 737–749; (d) Y. Huang, C. Pi, X. Cui and Y. Wu, *Adv. Synth. Catal.*, 2020, **362**, 1385–1390; (e) Q. Wang, Y. H. Nie, C. X. Liu, W. W. Zhang, Z. J. Wu, Q. Gu, C. Zheng and S.-L. You, *ACS Catal.*, 2022, **12**, 3083–3093; (f) L. Zhou, H. G. Cheng, L. Li, K. Wu, J. Hou, C. Jiao, S. Deng, Z. Liu, J. Q. Yu and Q. Zhou, *Nat. Chem.*, 2023, **15**, 815–823; (g) X. Kuang, J.-J. Li, T. Liu, C.-H. Ding, K. Wu, P. Wu and J.-Q. Yu, *Nat. Commun.*, 2023, **14**, 7698; (h) Q.-J. Yao, F.-R. Huang, J.-H. Chen and B.-F. Shi, *Nat. Commun.*, 2024, **15**, 7135; (i) J.-Y. Ma, Q.-J. Yao, L.-C. Jiang, F.-R. Huang, Q. Yue and B.-F. Shi, *J. Am. Chem. Soc.*, 2025, **147**, 7061–7069.
- (a) R. G. Array, J. Adrio and J. C. Carretero, *Angew. Chem., Int. Ed.*, 2006, **45**, 7674–7715; (b) K. Yoshida and R. Yasue, *Chem. – Eur. J.*, 2018, **24**, 18575–18586.
- (a) O. Riant, O. Samuel, T. Flessner, S. Taudien and H. B. Kagan, *J. Org. Chem.*, 1997, **62**, 6733–6745; (b) A. Urbano, G. Hernández-Torres, A. M. del Hoyo, A. Martínez-Carrión and M. C. Carreño, *Chem. Commun.*, 2016, **52**, 6419–6422; (c) C.-X. Liu, F. Zhao, Q. Gu and S.-L. You, *ACS Cent. Sci.*, 2023, **9**, 2036–2043.
- Z. Yu, Q. Liu, Q. Li, Z. Huang, Y. Yang and J. You, *Angew. Chem., Int. Ed.*, 2022, **61**, e202212079.
- (a) R. A. Thorat, Y. Mandhar, D. Parganiha, K. B. Patil, V. Singh, B. Shakir, S. Raju and S. Kumar, *ChemistrySelect*, 2023, **8**, e202203945; (b) R. A. Thorat, D. Parganiha, S. Jain, V. Choudhary, B. Shakir, K. Rohilla, R. K. Jha and S. Kumar, *Org. Lett.*, 2025, **27**, 552–558; (c) D. Parganiha, R. A. Thorat, A. D. Dhumale, Y. D. Upadhyay, R. K. Jha, S. Raju and S. Kumar, *Chem. Sci.*, 2025, **16**, 700–708.
- (a) J. M. González, X. Vidal, M. A. Ortuño, J. L. Mascareñas and M. Gulías, *J. Am. Chem. Soc.*, 2022, **144**, 21437–21442; (b) P. Losada, L. Goicoechea, J. L. Mascareñas and M. Gulías, *ACS Catal.*, 2023, **13**, 13994–13999.
- S. Mallick, T. Mandal, N. Kumari, L. Roy and S.-D. Sarkar, *Chem. – Eur. J.*, 2024, **30**, e202304002.
- J. Kim, G. Golime, H. Y. Kim and K. Oh, *Asian J. Org. Chem.*, 2019, **8**, 1674–1679.
- L. Chu, X. C. Wang, C. E. Moore, A. L. Rheingold and J. Q. Yu, *J. Am. Chem. Soc.*, 2013, **135**, 16344–16347.

